

Formation of the Ferritin Iron Mineral Occurs in Plastids¹

An X-Ray Absorption Spectroscopy Study

Geoffrey S. Waldo, Eric Wright, Zhi-Hai Whang, Jean-Francois Briat, Elizabeth C. Theil*, and Dale E. Sayers

Department of Physics and Biochemistry, North Carolina State University, Raleigh, North Carolina 27695 (G.S.W., E.W., Z.-H.W., E.C.T., D.E.S.); and Laboratoire de Biochimie et Physiologie Végétales, Centre National de la Recherche Scientifique (Unité de Recherche 573), Institut National de la Recherche Agronomique et Ecole Nationale Supérieure d'Agronomie PlaceViala, F.34060 Montpellier cedex 1, France (J.-F.B.)

Ferritin in plants is a nuclear-encoded, multisubunit protein found in plastids; an N-terminal transit peptide targets the protein to the plastid, but the site for formation of the ferritin Fe mineral is unknown. In biology, ferritin is required to concentrate Fe to levels needed by cells (approximately 10^{-7} M), far above the solubility of the free ion (10^{-18} M); the protein directs the reversible phase transition of the hydrated metal ion in solution to hydrated Fe-oxo mineral. Low phosphate characterizes the solid-phase Fe mineral in the center of ferritin of the cytosolic animal ferritin, but high phosphate is the hallmark of Fe mineral in prokaryotic ferritin and plant (pea [*Pisum sativum* L.] seed) ferritin. Earlier studies using x-ray absorption spectroscopy showed that high concentrations of phosphate present during ferritin mineralization in vitro altered the local structure of Fe in the ferritin mineral so that it mimicked the prokaryotic type, whether the protein was from animals or bacteria. The use of x-ray absorption spectroscopy to analyze the Fe environment in pea-seed ferritin now shows that the natural ferritin mineral in plants has an Fe-P interaction at 3.26 Å, similar to that of bacterial ferritin; phosphate also prevented formation of the longer Fe-Fe interactions at 3.5 Å found in animal ferritins or in pea-seed ferritin reconstituted without phosphate. Such results indicate that ferritin mineralization occurs in the plastid, where the phosphate content is higher; a corollary is the existence of a plastid Fe uptake system to allow the concentration of Fe in the ferritin mineral.

Among the events that have occurred during the evolution of plant cells and plastids is the redistribution of ferritin from the cytoplasm to the plastid (reviewed by Theil and Hase, 1993). Much of the Fe in leaves, for example, is in the plastid, where ferritin is observed in the proplastid, but decreases in the mature chloroplast (Theil and Hase, 1993), presumably because the Fe concentrated in ferritin is incorporated into Fe proteins such as Fds and the photosynthetic reaction centers. In animals, ferritin is mainly a cytoplasmic protein. Ferritin is required in biol-

ogy to concentrate Fe because of the low solubility of Fe (10^{-18} M) and the relatively high concentration of Fe needed by cells (10^{-7} M) (Theil, 1987).

Ferritin protein subunits in plants, encoded in the nucleus, are synthesized in the cytoplasm with a transit peptide that targets the protein to the plastid (Ragland et al., 1990). Ferritin in both plants and animals as well as bacteria is a multisubunit protein (reviewed by Theil, 1987, 1990; Harrison and Lilley, 1990; Waldo and Theil, 1995). A cage is formed by the subunits that directs the transportation of Fe ions and protons in and out of the mineral that forms in the hollow center of the protein. The mineral can have up to 4500 Fe atoms in various forms of hydrated ferric oxide. In plants, whether the mineralization of ferritin occurs before or after protein transport to the plastid is not known. If ferritin mineralization occurs after protein transport to the plastid, then the plastid must have an active system to take up Fe for incorporation into ferritin. Ferritin in plants has a high Fe:P ratio (Laulhére et al., 1989, 1992).

To investigate the site of ferritin mineralization in plants, advantage was taken of the effect of phosphate on the structure of the mineral formed in vitro in animal ferritin and on the mineral formed in vivo in ferritin of bacteria. EXAFS of ferritin minerals with a high phosphate content showed that phosphate was distributed throughout rather than on the surface (Rohrer et al., 1990). In addition, by comparing the EXAFS analysis of the mineral in animal ferritin reconstituted in the presence of high phosphate in vitro to the naturally high-phosphate mineral in *Azotobacter vinelandii*, EXAFS analysis can be used to show that the mineral structure in ferritin reflects the phosphate concentration present during mineralization in vivo (Rohrer et al., 1990). Long-range mineral structure in ferritin was also shown to be affected by the phosphate concentration when, with the use of high-resolution EM, *A. vinelandii* ferritin reconstituted without phosphate was observed to be like

¹ This work was partially supported by the National Institutes of Health (DK20251-ECT) and the U.S. Department of Energy (DE-FG05-89ER45384-DES). J.F.B. was supported by the Centre National de la Recherche Scientifique (ATIFE grant No. 93N60/0563).

* Corresponding author; e-mail elizabeth_theil@ncsu.edu; fax 1-919-515-5805.

Abbreviations: eV, electron volt; EXAFS, x-ray absorption spectroscopy; PSREC, Fe-reconstituted ferritin in the absence of added phosphate; PSREC plus P, Fe-reconstituted ferritin in the presence of added phosphate; k^3 , EXAFS data plotted to the third power; $k^3\chi$, Fourier transform data plotted to the third power; $\Delta\sigma^2$, the Debye-Waller factor relative to the standards; ν , standard variance between model and data.

natural horse-spleen ferritin (Mann et al., 1986). The EXAFS data also explained the long-range disorder previously observed in ferritin from bacteria (Mann et al., 1986) by showing that phosphate substituted for one or two of the Fe-O-Fe bridges, thus leading to smaller or more disordered Fe(III)-oxo complexes.

Since the phosphate concentration in plastids is higher than in the cytoplasm of plant cells (Bligny et al., 1990), as it is in the cytoplasm of prokaryotes, the short-range structure of the mineral in ferritin from plants could be used as a diagnostic tool to determine the site of mineralization. If, for example, phosphate could be shown by EXAFS to replace some of the Fe-O-Fe bridges in pea (*Pisum sativum* L.) seed ferritin mineral, as it does in ferritin from prokaryotes, then mineralization of ferritin occurred in the plastid. We now report that the mineral of pea-seed ferritin has an Fe-P environment like that of bacteria and that the short-range structure of the mineral in pea-seed ferritin protein depends on the phosphate concentration during mineralization. Thus, mineralization of ferritin in plants appears to occur in the plastid, which indicates that ferritin protein uptake by the plastid is distinct from, but possibly coordinated with, Fe uptake by the plastid.

MATERIALS AND METHODS

Native pea (*Pisum sativum* L.) seed plastid holo-ferritin was isolated from pea-seed tissue as previously described (Laulhère et al., 1989). The native pea-seed ferritin had an Fe content of approximately 1800 Fe atoms/molecule and an Fe:P ratio of 1.8. The holo-ferritin was dialyzed against buffer A (150 mM Mops, pH 7.0, 0.20 M NaCl) and concentrated by ultrafiltration in Amicon (Beverly, MA) PM-30 microconcentrators to 10 mg/mL. Apoferritin was prepared by extensive dialysis of 2 mL of the holo-ferritin (approximately 3 mg/mL) against 200 mL of 1% (v/v) thioglycolic acid in buffer B (Mes buffer, pH 6.5, 0.20 M NaCl), in a modification of the Fe-removal procedure previously described (Chasteen and Theil, 1982). The dialysis was performed in the dark, under argon, to minimize photoreductive damage. The dialysate was changed four times at 12-h intervals until the wine-colored Fe(II)-thioglycolate complex was undetectable by visual inspection. The ferritin was dialyzed against 200 mL of buffer B containing Chelex 100 (Sigma) and then against three changes of buffer A. Fe content was determined by reductive o-phenanthroline-Fe(II) assay on denatured protein. Ferritin protein concentrations were determined as previously described (Rohrer et al., 1990). The final apoferritin contained <1 Fe/ferritin molecule.

Fe reconstitution experiments were performed in the presence (PSREC plus P) and absence (PSREC) of added phosphate. During the Fe reconstitution experiments, the final concentration of protein was 2.08×10^{-6} M, and the intracellular $[\text{Fe}^{2+}]$ was 1.0×10^{-3} M in buffer A, in a reaction volume of 1 mL. The reaction was initiated by adding Fe(II) as a 50- μL aliquot of 20 mM FeSO_4 stock in 0.05 M HCl to the rapidly stirred protein solution. The resulting ratio of Fe/ferritin molecule was 480:1. The conditions for reconstitution of the apoferritin with Fe in the

presence of phosphate (PSREC plus P) were identical except that a 50- μL aliquot of 0.25 M K_2HPO_4 , pH 7.0, was added to a final concentration of 0.25×10^{-3} M 30 min prior to the addition of Fe(II). The Fe:P ratio (1:0.25) was the same as previously used so as to facilitate comparison with earlier studies (Rohrer et al., 1990). All reconstitution experiments were performed at ambient temperature (approximately 27°C) and under ambient oxygen concentration (approximately 2.5×10^{-4} M). The reconstituted ferritins were allowed to incubate for 6 h at approximately 27°C and then stored for 48 h at 4°C prior to being concentrated 5-fold to a final Fe concentration of 5 mM in Amicon PM-30 microconcentrators. Ferritin samples (native pea seed, PSREC, PSREC plus P) were loaded into 60- μL Lucite cells equipped with 6- μm polypropylene windows immediately before measurement of x-ray absorption data.

X-ray absorption data were obtained at ambient temperature at the National Synchrotron Light Source (Upton, NY), on beamline XII-A in fluorescence mode, using a 13-element Ge array detector. Six to eight 45-min scans were measured and averaged for each sample. Background removal was accomplished by calculating an optimum spline over the range 3 to 11 $\text{k}(\text{\AA}^{-1})$ using an automatic spline background removal program. The criteria and approach used in the background removal were as previously described (Cook and Sayers, 1981). The k^3 -weighted EXAFS were modeled as previously described (Islam et al., 1989; Rohrer et al., 1990) using Fe (NO_3)₃ as a model for Fe-O (6O at 1.99 Å), Fe(II)-O as a model for Fe-Fe (12 Fe at 3.05 Å), and $\text{FePO}_4 \cdot 7\text{H}_2\text{O}$ as a model for Fe-P (4 P at 3.33 Å). All standards were measured as powders in the transmission mode, except for $\text{Fe}(\text{NO}_3)_3$, which was measured at a concentration of 0.05 M in 0.1 M HNO_3 in fluorescence mode.

In the tables, ν is a quantitative measure of the difference between the refined model and the data. The uncertainty in a given parameter was determined by fixing all other parameters at the optimal values and conducting a grid search about the given parameter until the overall ν doubled. In initial fits, the data were filtered to isolate a given shell of scatterers by inverse Fourier transformation. In other fits, a wide window was selected to include all of the shells for the inverse transform.

RESULTS

X-ray absorption near-edge spectra for native, PSREC, and PSREC plus P are shown in Figure 1. The spectra can essentially be superimposed, and in each case the area ($7.5 \pm 0.5 \times 10^{-2}$ eV) of the pre-edge feature at approximately 7116 eV associated with the $1s \rightarrow 3d$ transition is consistent with a centrosymmetric six-coordinate environment about the central Fe(III) atom ($1s \rightarrow 3d$ areas range from 5.8 to 9.3×10^{-2} eV for 6-coordinate Fe environments) (Roe et al., 1984). The k^3 -weighted EXAFS are shown in Figure 2A, and the corresponding Fourier transforms are shown in Figure 2B. Note the larger amplitude at 3.5 Å at longer distances in the pea-seed ferritin reconstituted without P (Fig. 2B, b). Similar results were obtained with natural horse-spleen ferritin that has a low P content (Rohrer et al., 1990).

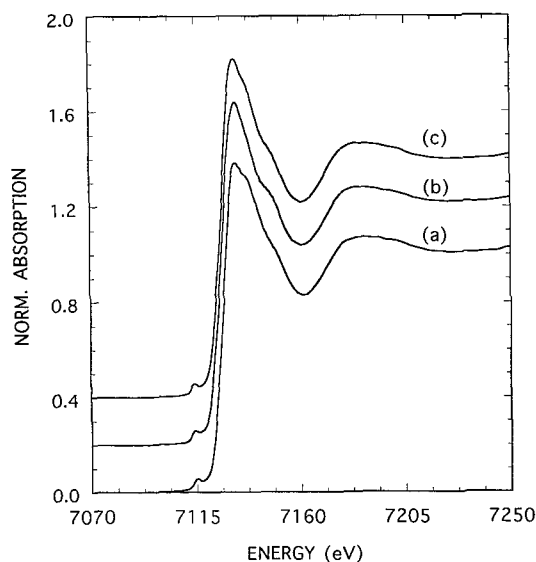


Figure 1. Normalized x-ray absorption near-edge spectra for native pea-seed ferritin; a, PSREC; b and c, PSREC plus P.

Natural pea-seed ferritin and pea-seed ferritin reconstituted with P are similar to each other (Fig. 2, A and B, a and c) and to bacterial ferritin (Rohrer et al., 1990).

Nearest-Neighbor Fe-O/N Scatterers

To isolate the first shell of scatterers, the Fourier transform data in Figure 2B were backtransformed over the range 0.5 to 2.0 Å. In agreement with previous results for bacterial and mammalian ferritins (Rohrer et al., 1990), the first shell of (O/N) neighbors in all of the samples could be modeled by a single shell of five to six low-Z atoms (O/N) at approximately 1.95 to 1.97 Å. Using a split shell of two Fe-(O/N) distances resulted in no improvement in the quality of the fit for any of the samples, indicating that the presence of P did not result in a detectable second-shell Fe-(O/N) distance. The results summarized in Table I show that the presence of P had no effect on the first shell of scatterers, since none of the samples are distinguishable by EXAFS. The presence of phosphate in PSREC plus P resulted in greenish-brown cores, as previously noted for mammalian ferritins reconstituted with Fe in the presence of phosphate (Rohrer et al., 1990). In contrast PSREC had the usual brownish, rust-colored appearance of low-phosphate ferritin.

Fe-P and Fe-Fe Scatterers

Fe-Fe and Fe-P scattering were isolated by backtransforming the Fourier transform data in Figure 2B over the range 2.3 to 3.3 Å. The resulting EXAFS data are shown in Figure 3. Although the Fe-Fe- and Fe-P-scattering distances are too similar to be resolved into separate shells, the phase and amplitude functions of the two elements are distinctive enough to allow the modeling of Fe-P scattering in the presence of Fe-Fe interactions (Mansour et al., 1985; Hedman et al., 1986; Rohrer et al., 1990). Various single-shell

fits were tried with Fe-(O/N), Fe-Fe, and Fe-P as models; none modeled the data acceptably. In the case of native pea-seed ferritin and PSREC plus P, fits using Fe-Fe or Fe-P alone, either as single- or two-shell fits, resulted in a poor model. An improvement of more than 10-fold in the quality of the fit (as judged by the ν) resulted when Fe-Fe and Fe-P were used in a two-shell fit. (For a discussion of evaluating the uniqueness of the fit, see Mansour et al. [1985].) In

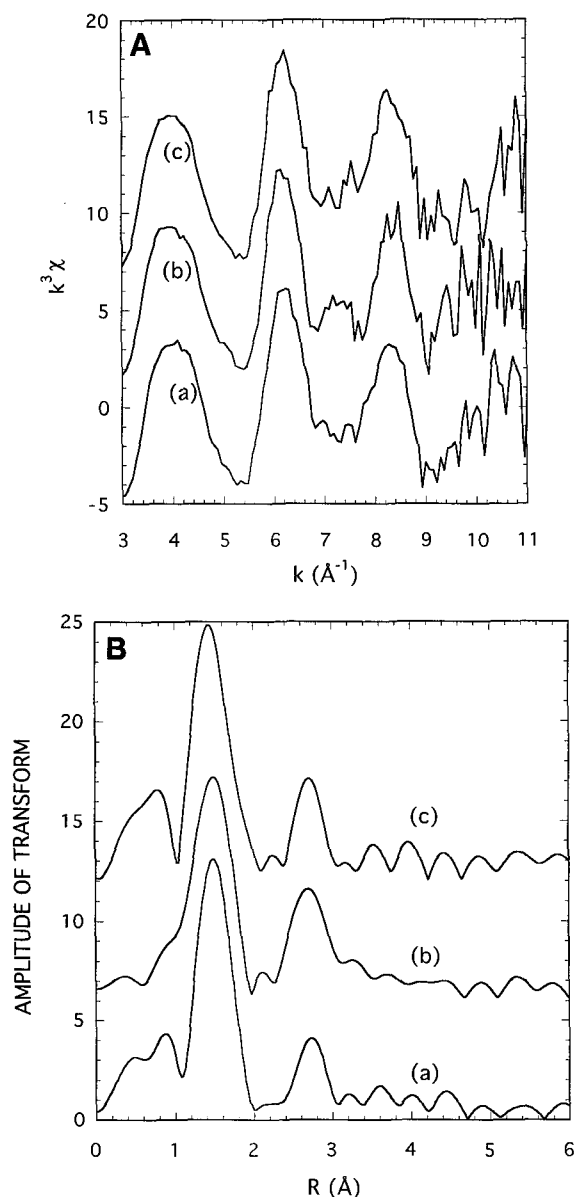


Figure 2. A, k^3 -weighted EXAFS of native pea-seed ferritin (a), PSREC (b), and PSREC plus P (c). Note the intensity of the spectrum in the region 6.8 to 7.5 $k(\text{Å}^{-1})$ for b, suggesting a stronger Fe-Fe interaction, which is supported by the EXAFS analysis (Table II). B, Fourier transforms of k^3 -weighted EXAFS in A in the range of 3 to 11 Å^{-1} for native pea-seed ferritin (a), PSREC (b), and PSREC plus P (c). Note that data for PSREC are comparable to those for natural horse-spleen ferritin and horse-spleen ferritin reconstituted without phosphate (Brown et al., 1979; Rohrer et al., 1990).

Table I. Fe-(O/N) nearest-neighbor scatters in ferritin with and without phosphate

The fitting ranges in the Fourier transforms were 0.5 to 2.0 Å for the plant ferritin samples. κ^3 weighting was used and the data were analyzed over the range 3 to 11 Å⁻¹, using the approach described previously; see Islam (1989) and "Materials and Methods."

Sample	CN ^a	$r(\text{Å})^b$	$\Delta\sigma^2 \times 10^3 (\text{Å}^2)^c$	$\Delta E (\text{eV})^d$	v^e
Native Pea Seed ^f	5.5 ± 0.5	1.97 ± 0.05	1.6 ± 0.2	1 ± 1.5	0.182
Fe:P = 1:0; PSREC ^g	5.5 ± 0.5	1.96 ± 0.03	4.8 ± 0.8	3.6 ± 1	0.266
Fe:P + 1:0.25; PSREC + P ^g	5.5 ± 0.5	1.95 ± 0.04	1.4 ± 0.3	4.6 ± 4	0.428
AV ferritin ^h	5.5 ± 0.5	1.95 ± 0.05	5.44 ± 0.5	3.50 ± 1	0.31 × 10 ⁻⁵

^a CN, Coordination number or number of scatterers at a given distance from the central Fe atom. ^b r , The interatomic distance. ^c $\Delta\sigma^2$, is a measure of disorder in the structure (Brown et al., 1979; Islam et al., 1989). ^d ΔE , The shift of the energy origin of the data relative to that of the standard during refinement. ^e The variance reported for *A. vinelandii* is for κ^0 weighting. ^f Native pea-seed ferritin isolated from pea seed plastids (Laulhére et al., 1992). ^g The pea-seed protein coats reconstituted with 480 Fe atoms/molecule in the absence (PSREC) or presence (PSREC + ΔP) of K₂HPO₄. ^h Data for *A. vinelandii* (AV) bacterial ferritin (Rohrer et al., 1990).

contrast, no improvement in the model for PSREC resulted when Fe-P was included, either alone or in combination with other shells of Fe, P, or (O/N). Instead, the data from 2.01 to 3.55 Å for PSREC was best modeled with two shells of Fe-Fe scatterers at 3.08 and 3.52 Å, respectively. Plots of the backtransform (Fig. 3) show the influence of P, which replaces one of the Fe-Fe distances in ferritin minerals high in P. For natural pea ferritin and PSREC plus P the shape is clearly a mixture of contributions from low- and high-Z neighbors (Fe-P). In contrast, the backtransform for PSREC has the shape characteristic of contributions predominantly from a high-Z (Fe plus S) scatterer.

The parameters derived from the optimal fits to the data from 2.01 to 3.55 Å are summarized in Table II. Overall, the fitting results for the high-phosphate mineral cores are consistent with those reported previously for native bacterial ferritin and mammalian ferritins reconstituted in the presence of phosphate (Rohrer et al., 1990). The first-shell scatterers at approximately 1.96 Å were indistinguishable by EXAFS for both the high- and low-phosphate minerals (see Table I). Animal ferritin or low-phosphate ferritins

have an Fe-Fe interaction at 3.0 and 3.5 Å. Phosphate oxygen substitutes for a subset of the nearest-neighbor Fe-bridging oxo groups, since phosphorus at approximately 3.2 Å replaces many of the Fe-Fe scatterers at 3.08 Å in the native pea-seed and PSREC plus P samples (Table II), as judged by a coordination number of 2 compared to 4 when phosphate is absent. Fe-Fe scattering at 3.5 Å was not observed in the high-phosphate mineral cores, indicating a larger disorder in the long-range Fe-Fe interactions (3.5 Å) than in the Fe-Fe interactions at 3.08 Å for pea-seed ferritin. A significant peak between 6.6 and 7.6 Å⁻¹ in the $\kappa^3 \chi$ data is observed only in pea-seed ferritin (PSREC) reconstituted without phosphate (Fig. 2A, b); the area under the peak in the Fourier transform between 2.01 and 3.50 is also larger in PSREC (Fig. 2B, b). Since EXAFS measures all of the Fe in the mineral core, the results further indicate that the phosphate is distributed throughout the entire core rather than being localized at a small subset of surface sites or lattice defects. Why it is that the longer Fe-Fe interaction (3.5 Å) is more disordered in plant ferritin and the shorter Fe-Fe interaction is more disordered in bacterial ferritin is not clear, but this observation suggests a subtle influence of the protein in addition to the environmental phosphate.

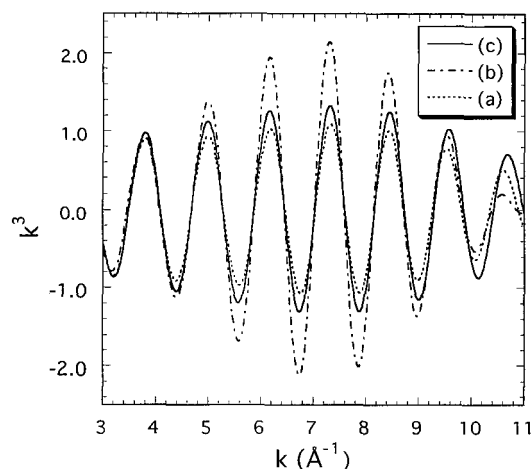


Figure 3. Inverse Fourier transforms of spectra in Figure 2B in the range of 2.3 to 3.3 Å. a, Native pea-seed ferritin; b, PSREC; c, PSREC plus P. The shape of the curve for b is indicative of more ordered Fe-Fe interactions, whereas the shape of the curves for a and c are characteristic of mixtures of species, which is supported by the quantitative analysis.

DISCUSSION

The relatively high phosphate concentration in plastids and the cytoplasm of prokaryotes can explain the amount and the location of phosphate in the structure of the ferritin mineral from plants and bacteria. For example, chloroplast Pi concentrations are 12 mM (Bligny et al., 1990), whereas cytoplasmic Pi concentrations are much lower and are estimated to be approximately 1 mM (Roby et al., 1987; Bligny et al., 1990). The ferritin mineral is structurally indistinguishable from natural mineral (P:Fe = 1:1) and reconstituted mineral (P:Fe = 1:4) but is clearly distinctive compared to the high-phosphate minerals formed in vivo or in vitro, in which the P:Fe ≤ 8:1 (Rohrer et al., 1990). The similarity of the ferritin Fe mineral in natural ferritin from pea seed, the bacterium *A. vinelandii* (Table II; Rohrer et al., 1990), and horse-spleen ferritin reconstituted in the presence of high phosphate (P:Fe = 1:4) indicates that the presence of phosphate in the environment supplying the ferritin with Fe dominates over variations in amino acid

Table II. EXAFS analysis of Fe-Fe and Fe-P scatterers for ferritins with and without large amounts of phosphate

The fitting ranges in the Fourier transforms were 2.3 to 3.3 Å for the plant ferritin samples. κ^3 weighting was used and the data were analyzed over the range 3 to 11 Å⁻¹; see Islam (1989) and "Materials and Methods."

Sample	CN ^a	$r(\text{Å})^b$	$\Delta\sigma^2 \times 10^3 (\text{Å}^2)^c$	$\Delta E (\text{eV})^d$	$\nu \times 10^{1e}$
P neighbors					
Native pea seed ^f	4.0 ± 0.5	3.26 ± 0.02	-5.1 ± 0.3	-2.5 ± 2	0.28
Fe:P = 1:0.25; PSREC + P ^g	4.0 ± 0.5	3.27 ± 0.03	-7.9 ± 0.3	-1.4 ± 2	0.66
AV ferritin ^h	5.0 ± 1.0	3.17 ± 0.04	-2.6 ± 0.1	3.7 ± 0.5	0.24
Fe neighbors					
Native pea seed ^f	2.0 ± 0.5	3.08 ± 0.02	-3.9 ± 0.4	-12.4 ± 1	0.28
Fe:P = 1:0.25; PSREC + P ^g	2.0 ± 0.5	3.07 ± 0.04	-9.0 ± 0.3	-12.3 ± 2	0.66
Fe:P = 1:0; PSREC ^g	4.0 ± 0.4	3.08 ± 0.03	-8.2 ± 0.8	-8.2 ± 2	0.86
	2.0 ± 0.5	3.52 ± 0.06	-5.6 ± 0.4	-7.9 ± 1	0.86
AV ferritin ^h	1.6 ± 0.8	3.50 ± 0.02	0.79 ± 0.05	1.11 ± 2	0.24 × 10 ⁻⁶

^a CN, Coordination number or number of scatterers at a given distance from the central Fe atom. ^b r , The interatomic distance. ^c $\Delta\sigma^2$ is a measure of disorder in the structure (Brown et al., 1979; Islam et al., 1989). ^d ΔE , The shift of the energy origin of the data relative to that of the standard during refinement. ^e The ν in the model is data reported for *A. vinelandii* is for κ^0 weighting. ^f Native pea-seed ferritin isolated from pea seed plastids (Laulhère et al., 1992). ^g The pea-seed protein coats reconstituted with 480 Fe atoms/molecule in the presence (PSREC + P) or absence (PSREC) of K₂HPO₄. Two-shell fits with Fe, P resulted in variances at least 10-fold better than for single-shell fits or two-shell Fe fits. Data could not be modeled successfully by interchanging Fe and P distances in fits using two-shell models. ^h Data for *A. vinelandii* (AV) bacterial ferritin (Rohrer et al., 1990).

sequence for determining the structure of the mature mineral core.

Ferritin is required in biology to concentrate Fe above the concentration possible for the free ion (10⁻¹⁸ M) to match the Fe requirement of cells (approximately 10⁻⁷ M) (Theil, 1987). The Fe is stored as a solid in the center of the multisubunit protein coat. Ferritin protein is the only known example of a protein that controls the reversible phase transition of a metal ion in solution to a solid, but it can be a model for supramolecular complexes such as the extracellular matrix and those formed by cells that participate in the formation or remodeling of Ca and phosphate in teeth and bone. Whether variations in ferritin mineral have physiological significance, such as storing phosphate, remains unknown.

EXAFS analysis showed a decrease in short-range order in the high-phosphate pea-seed ferritin mineral cores, compared to low-phosphate animal ferritins. The greater disorder in the pea-seed ferritin mineral provides an explanation of the lower hyperfine field (445 ± 2 kilooersteds) (Wade et al., 1993) relative to low-phosphate animal ferritins (Mann et al., 1986), the magnetic ordering at 4.1 K (Bauminger et al., 1980; Wade et al., 1993), the amorphous morphology of the pea-seed cores as seen by EM, and the absence of lattice fringes by electron diffraction (Wade et al., 1993).

The resemblance of native plant and bacterial ferritin cores mineralized in vivo, as determined by EXAFS (Table II; Rohrer et al., 1990), shows that ferritin in plants combines prokaryotic features of the mineral with the eukaryotic features of the protein sequence and nuclear encoding of the gene (Ragland et al., 1990). Prokaryotic features of the pea-seed ferritin mineral structure (Table II) indicate that plant ferritin is mineralized after translocation of the protein to the plastid, where the phosphate concentration that influences the mineral structure is high. Ferritin can

thus be added to the group of nuclear-encoded, plastid metalloproteins such as plastocyanin and Fd (Merchant and Bogarad, 1986; Li et al., 1990), which share the property of assembly of the protein metal complex in the plastid. Moreover, plastids must have an active mechanism for taking up the Fe that is concentrated in ferritin; the mechanism of Fe uptake by plastids remains to be clarified.

Received February 28, 1995; accepted June 30, 1995.

Copyright Clearance Center: 0032-0889/95/109/0797/06.

LITERATURE CITED

- Bauminger ER, Cohen SG, Dickson DPE, Levy A, Ofer S, Yariv J (1980) Mössbauer spectroscopy of *E. coli* and its iron storage protein. *Biochim Biophys Acta* **623**: 237-242
- Bligny R, Gardestrom P, Roby C, Douce R (1990) ³¹P NMR studies of spinach leaves and their chloroplasts. *J Biol Chem* **265**: 1319-1326
- Brown MA, Theil EC, Sayers DE (1979) Similarity of the structure of ferritin and iron-dextran (imferon) determined by extended x-ray absorption fine structure Analysis. *J Biol Chem* **254**: 8132
- Chasteen ND, Theil EC (1982) Iron binding by horse spleen apoferritin: a vanadyl(IV) EPR spin probe study. *J Biol Chem* **257**: 7672-7677
- Cook JW, Sayers DE (1981) Criteria for automatic EXAFS background removal. *J Appl Physiol* **52**: 5024
- Harrison PM, Lilley TH (1990) Ferritin. In TM Loehr, ed, *Iron Carriers and Iron Proteins*. VCH, New York, pp 353-452
- Hedman B, Co MS, Armstrong WL, Hodgson KO, Lippard SJ (1986) EXAFS studies of binuclear iron complexes as models for binuclear iron complexes and related compounds. *Inorganic Chemistry* **25**: 3708-3714
- Islam QT, Sayers DE, Gorun SM, Theil EC (1989) A model for an intermediate stage in the formation of the ferritin iron core. *J Inorg Biochem* **36**: 51-62
- Laulhère JP, Laboure AM, Briat JF (1989) Mechanism of the transition from plant ferritin to phyto-siderin. *J Biol Chem* **264**: 3629-3635
- Laulhère JP, Laboure AM, Van Wuytswinkel O, Gagnon J, Briat JF (1992) Purification, characterization and function of bacterio-

- ferritin from *Cyanobacterium pynechocystis* P.C.C.6803. *Biochem J* **281**: 785–793
- Li HM, Theg SM, Bauerle CM, Keegstra K** (1990) Metal ion-center assembly of ferredoxin and plastocyanin in isolated chloroplasts. *Proc Natl Acad Sci USA* **87**: 6748–6752
- Mann S, Bannister JV, Williams RJP** (1986) Structure and composition of ferritin cores isolated from human spleen Limpet (*Patella vulgaris*) and bacterial (*Pseudomonas aeruginosa*) cells. *J Mol Biol* **188**: 225–232
- Mansour AN, Thompson C, Theil EC, Chasteen ND, Sayers DE** (1985) Fe(III)-ATP complexes: models for ferritin and other polynuclear iron complexes with phosphate. *J Biol Chem* **260**: 7975–7979
- Merchant S, Bogarad L** (1986) Rapid degradation of apoplastocyanin in Cu(II) deficient cells of *Chlamydomonas reinhardtii*. *J Biol Chem* **261**: 15850–15853
- Ragland M, Briat JF, Gagnon J, Laulhère JP, Massenet O, Theil EC** (1990) Evidence for conservation of ferritin sequences among plants and animals and for a transit peptide in soybean. *J Biol Chem* **263**: 18339–18344
- Roby C, Martin J-B, Bligny R, Douce R** (1987) Biochemical changes during sucrose deprivation in higher plant cells. *J Biol Chem* **262**: 5000–5007
- Roe AL, Schneider DJ, Mayer RJ, Pyrz JW, Widom J, Que L Jr** (1984) X-ray absorption spectroscopy of iron tyrosinate proteins. *J Am Chem Soc* **106**: 1676–1681
- Rohrer JS, Islam QT, Watt GD, Sayers DE, Theil EC** (1990) The iron environment in ferritin with large amounts of phosphate, from *Azotobacter vinelandii* and horse spleen, analyzed using extended x-ray absorption fine structure (EXAFS). *Biochemistry* **29**: 259–264
- Theil EC** (1987) Ferritin: structure, gene regulation, and cellular function in animals, plants, and microorganisms. *Annu Rev Biochem* **56**: 289–315
- Theil EC** (1990) The ferritin family of iron storage proteins. *Adv Enzymol Relat Areas Mol Biol* **63**: 421–449
- Theil EC, Hase T** (1993) Plant and microbial ferritins. In *Iron Chelation in Plants and Soil Microorganisms*, Vol 5. Academic Press, San Diego, CA, pp 133–156
- Wade VJ, Treffry A, Laulhère JP, Bauminger ER, Cleton MI, Mann S, Briat JF, Harrison PM** (1993) Structure and composition of ferritin cores from pea seed (*Pisum sativum*). *Biochim Biophys Acta* **1161**: 91–96
- Waldo GS, Theil EC** (1995) Ferritin and iron biomineralization. In *KS Suslick, ed, Comprehensive Supramolecular Chemistry, Bioinorganic Systems*, Vol 5. Pergamon Press, Oxford, UK (in press)